SAXS from Polyelectrolyte Solutions under Shear: Xanthan and Na−Hyaluronate Examples†

M. Villetti,# R. Borsali,*,‡ O. Diat,§ V. Soldi,# and K. Fukada⊥

LCPO-CNRS-ENSCPB Bordeaux University (UMR 5629), Avenue Pey-Berland, BP 108-33402 Talence, Cedex, France, and Universidade Federal de Santa Catarina, Departamento de Quimica, Florianopolis 88040-900 Santa Catarina, Brazil

Received June 2, 2000; Revised Manuscript Received September 25, 2000

ABSTRACT: Xanthan and Na−hyaluronate (Na−Hy) polysaccharides belong to a class of polyelectrolytes that show a maximum in the reduced viscosity as a function of polyelectrolyte concentration. It is also well documented that xanthan solutions present a polyelectrolyte scattering maximum as a function of the wavevector *q*. However, despite considerable expanded experimental efforts, no scattering peak was observed in Na−Hy systems when using light or neutron scattering techniques. *In this work and for the first time, we report that only the use of high brilliance of synchrotron radiation at rest and under shear enables to highlight the expected small-angle scattering peak in the Na−Hy polyelectrolyte system.* At zero shear rate, the scattering profile reveals a very diffuse and hardly detectable maximum at ideal experimental conditions (i.e., semidilute "salt-free" polyelectrolyte concentration—or low ionic strength—and momentum transfer *q*). As the shear rate is increased, this very small maximum is magnified and reveals clearly the expected polyelectrolyte nature of Na−Hy not yet observed using other radiation (light or neutrons). The system undergoes a typical and progressive change from isotropic to anisotropic phase, when increasing the shear, confirming the origin of the peak and the role of the electrostatic interactions on the structural order in polyelectrolyte systems. These results are compared to those obtained under the same conditions on the xanthan polyelectrolyte system where, in addition to the so-called polyelectrolyte scattering peak, a second-order peak in the scattering profile is observed as a consequence of the shear.

Introduction

The presence of charges along polyelectrolyte chains modifies significantly their properties with respect to neutral polymers. During the past decades, considerable interest has been given to the properties of flexible and semiflexible polyelectrolyte systems from both theoretical and experimental points of view.[1−5] The recent theoretical studies were based on models including the concept of electrostatic persistence length,[6−8] double screening,[9] notion of correlation hole,[10] counterion condensation,[11] random phase approximation,[12,13] etc. Experimentally, flexible (such as NaPSS) and semiflexible (such as xanthan, hyaluronate, etc.) polyelectrolyte chains, in the absence of added salt or at low ionic strength, present a peculiar behavior with respect to their viscosity data. Above a certain concentration (in semidilute and concentrated regimes) denoted $C_{P\max}$, the reduced viscosity $\eta_r = (\eta - \eta_0)/(\eta_0 C_P)$, where η_0 is the solvent viscosity, increases when the polyelectrolyte concentration C_P decreases. This abnormal concentration dependence, in contrast to ordinary polymer solution behavior, is described by the empirical Fuoss law:[14]

$$\eta_r = \frac{A}{1 + BC_P^{1/2}} \tag{1}$$

where the constants A and B depend on the molecular weight M_w and the charge Z of the polymer. This equation summarizes quite well the behavior of η_r in the semidilute regime although it has no fundamental theoretical basis. Many experiments[15−19] carried out by different authors from different laboratories have indeed confirmed such a behavior in different polyelectrolyte systems.

On the other hand, the scattering intensity in polyelectrolyte "salt-free" systems is well documented and presents a maximum at a certain wavevector position, denoted by q^*, where $q = (4\pi/\lambda)\sin(\theta/2)$, λ is the wavelength of the incident beam, and θ is the scattering angle. As has been shown by several experimental studies, q^* scales with the polyelectrolyte concentration as $C_P^{1/2}$ in the semidilute regime and as $C_P^{1/3}$ in the dilute regime. This maximum of the scattering intensity disappears progressively when salt is added and therefore is interpreted as a consequence of electrostatic interactions. These interactions "impose" a preferential distance between charged particles and lead to "pseudo-organized" structures having uniform arrangement ($q^* \approx C_P^{1/3}$) in dilute regime and cylindrical or hexagonal packing ($q^* \approx C_P^{1/2}$) in the semidilute domain. Other work as described by Ise[2] shows that charged systems may be considered as formed by a two-state domain (ordered and disordered states). This description is supported by the existence of an upturn of the scattered intensity at small q range, the identification of a slow mode reported by many authors when using dynamic light scattering (DLS) in polyelectrolyte systems, and

* Corresponding author: E-mail: borsali@enscpb.u-bordeaux.fr.
† This work has been started at CERMAV (Grenoble).
‡ LCPO-CNRS-ENSCPB Bordeaux University.
# Universidade Federal de Santa Catarina.
§ CEA-CNRS Université J.Fourier DSM/DRFMC/SI3M/PCI, UMR 5819, 17 av. des Martyrs, 38054 Grenoble, Cedex 9, France.
⊥ Department of Chemistry, Graduate School of Science, Tokyo Metropolitan University, Minamiohsawa 1-1, Hachiohji, Tokyo 192-0397 Japan.

10.1021/ma000971z CCC: $19.00
Published on Web 11/18/2000

also the fact that the equivalent interparticle distance $D = (2\pi/q^*)$ is such as D(experimental) > D(calculated). One notes that, regarding the origin of the upturn, it has been discussed in more detail recently by Borsali et al.[20] on DNA solutions and by Ermi and Amis[21] on PMVP (poly-*N*-methyl-2-vinylpyridinium chloride) using combined small-angle neutron scattering (SANS) and static and dynamic light scattering (DLS) experiments.

Various experimental techniques[22−37] have been used to emphasize the behavior of such charged complex systems including small-angle X-ray and neutron scattering (SAXS and SANS, respectively), elastic and DLS, and viscosity measurements. Depending on the range of concentration, these experiments have shown indeed the existence of a maximum in the scattered intensity for "salt-free" solution or at low ionic strength. This has been observed for instance in the case of poly(styrenesulfonate) (NaPSS)[25,26] and polysaccharides[31,36,37] (succinoglycan and xanthan) when using light and neutron scattering experiments. In all those studies, it has been shown that the addition of a simple electrolyte (for instance, NaCl) to the solutions screens out the electrostatic interactions, and the maximum disappears progressively. It is however not yet clear whether the peak position remains constant or changes with the addition of salt since contradictory results[20,34] exist in the literature. More experimental investigations are certainly needed to shed some light on the effect of salt concentration on the position of the maximum.

In the case of Na−hyaluronate and in contrast to other polyelectrolyte systems, so far no light, X-rays, or neutron scattering peak was yet observed. Many reasons were invoked to explain the "nonexistence" of the scattering peak (as a matter of fact, it is the nonobservable peak as discussed below), namely, small persistence length, weakly charged system, weak scattered signal, etc. In this work we have carried out SAXS at the European Synchrotron Radiation Facility (ESRF, Grenoble) on xanthan and hyaluronate "salt-free" semidilute systems, at rest (zero shear) and at different shear rates. This has been achieved in order to gain more understanding of the electrostatic nature of these systems and also to highlight the existence or the nonexistence of the scattering peak in the case of Na−hyaluronate.

Experimental Section

Sample Description. The charged polysaccharide sodium hyaluronate (Hy, hyaluronate, hyaluronic acid) was provided by Shiseido Basic Research Lab. (Yokohama, Japan). This polysaccharide is found in the extra cellular matrix of mammals, whose molecular structure consists of a repeating disaccharide unit, D-glucaronic acid and *N*-acetyl-D-glucosamine. It was isolated from a strain of bacteria, *Streptococcus zooepidemicus*, that produces hyaluronic acid extracellularly and was highly purified according to Asakawa et al.'s method.[38] At neutral pH, it is soluble in water and behaves as a weakly charged polyelectrolyte due to the carboxylate group on each disaccharide unit. Hyaluronate in aqueous salt solutions is a wormlike chain characterized by an intrinsic persistence length ranging between 45 and 90 Å.[18,28,39] More recent light scattering results obtained by Villetti et al.[40] show that the intrinsic persistence length is about 70 Å. The system was characterized in 0.3 M NaCl by light scattering (ALV), viscosity (Ubbelohde capillary viscometer), and gel permeation chromatography (TSKgel 6000 PWXL, Tosoh Co., Japan). The molecular weight of the sample was identified to be 1.4×10^6 according to[39] $[\eta] = 0.0228M^{0.816}$ at 25 °C. This result is in good agreement with the light scattering data[40] which gave $\langle M\rangle_w = 1.37 \times 10^6$, radius of gyration $R_g = 1274$ Å, and second virial coefficient $A_2 = 1.52 \times 10^{-3}$ mol cm^3/g^2.

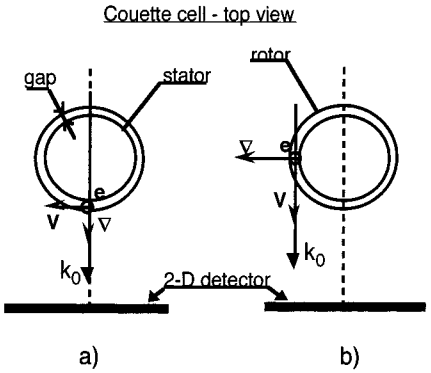

Figure 1. Schematic Couette cell setup at the ESRF, ID2 beamline: radial (a) and tangential (b) configurations.

The xanthan sample was provided by SKW Biosystems and purified following classical procedures. Light scattering experiments gave $\langle M\rangle_w = 8.59 \times 10^5$, $R_g = 1063$ Å, and $A_2 = 5.87 \times 10^{-4}$ mol cm^3/g^2. An estimate of error on the light scattering data for $\langle M\rangle_w$, R_g, and A_2 is about 3%.

Small-Angle X-ray Scattering. A series of small-angle X-ray scattering (SAXS) experiments were performed on the High Brilliance beamline ID2 at the ESRF.[41] The SAXS setup is based on a pinhole camera with a beamstop placed in front of a two-dimensional (2-D) gas-filled detector. The X-ray scattering patterns were recorded on the detector which was located at 6 m from the sample, using a monochromatic incident X-ray beam (1 Å wavelength) with a cross section of 0.2×0.2 mm^2 (V × H) at the sample position. The shearing device was a homemade (ESRF) polycarbonate Couette cell. The rotor is the outer cylinder (22 mm in diameter), and the size of the annular gap between both cylinders of the cell is 1 mm. Of major importance for the present experiment is that the shearing cell is mounted on motorized translation stages which allow the sample to be aligned in any beam-path positions between the so-called radial and tangential positions. Both experimental configurations are illustrated in parts a and b of Figure 1, respectively. The first one (radial configuration) corresponds to $\mathbf{k}0//\nabla$, the velocity gradient, and the second one (tangential configuration) to $\mathbf{k}0//\mathbf{V}$ the shear velocity, where $\mathbf{k}0$ is the incident X-ray wave vector. The third direction is defined by the unit vector $\mathbf{e} = \mathbf{V} \times \nabla$ which is usually called vorticity. These configurations are essential since for layered structures or ordered systems they provide the structure factor in two perpendicular planes of the reciprocal lattice, namely the ($\mathbf{k}$v,$\mathbf{k}$e) and the ($\mathbf{k}\nabla$,$\mathbf{k}$e) planes. The set of these three vectors $\mathbf{k}$i is actually fixed by the flow conditions of the cell. The beam size being smaller than the gap size, we can also scan through the gap in the gradient velocity direction. The raw data have been normalized by the transmission (measured online) and corrected by the response of the 2D detector. The investigated range of the shear was from $\dot\gamma = 0.05$ s^{-1} to $\dot\gamma = 1600$ s^{-1}.

Results and Discussion

At rest (zero shear rate), all investigated "salt-free" xanthan concentrations in the semidilute regime ranging from 5 g/L < C_P < 30 g/L showed scattering peaks whose positions q^* scales as $C_P^{1/2}$. On the other hand, "salt-free" Na−Hy did show a very small and broad maximum in $I(q)$ vs q. This behavior is illustrated in Figure 2 where the scattered intensity $I(q)$ vs q for Na−Hy and xanthan are plotted at the same concentration 15 g/L. For the xanthan case, the peak is very well developed, and its position is in perfect agreement with earlier neutron scattering results.[37] As for the Na−Hy system, there is a very small maximum when $I(q)$ is plotted in another scale as shown in the inset of Figure 2. As compared to other experiments[40] (light and neutron scattering) where not even any "shoulder" was

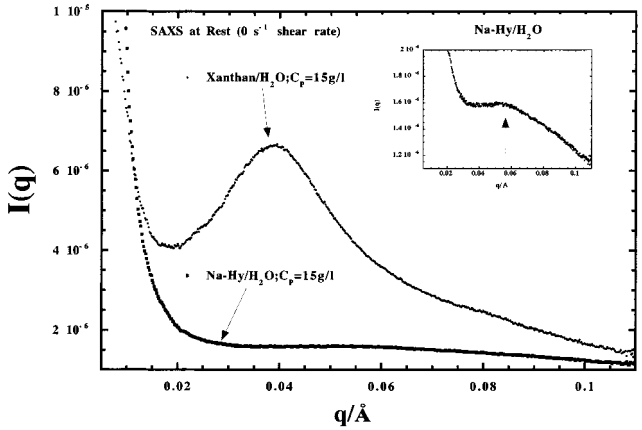

Figure 2. $I(q)$ vs q at rest (zero shear rate) for the xanthan and Na−hyaluronate samples at polyelectrolyte "salt-free" concentration $C_P = 15$ g/L. Distance sample-to-detector $L = 6$ m, X-ray wavelength $\lambda = 1$ Å. The inset refers to the Na−Hy system plotted at a different scale.

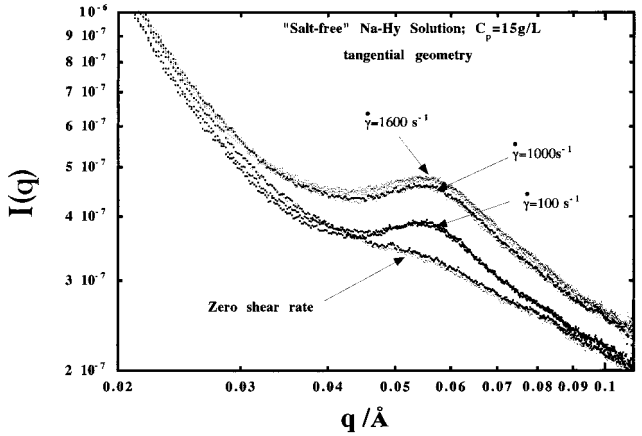

Figure 3. $I(q)$ vs q for the Na−hyaluronate sample at the polyelectrolyte "salt-free" concentration $C_P = 15$ g/L in the tangential geometry at rest and at different shear rates (from $\dot{\gamma} = 0.05$ s^{-1} to $\dot{\gamma} = 1600$ s^{-1}). Note that the peak position does not change with the shear.

reported, the difference with the present SAXS experiments is indeed the high brilliance which allowed the observation of this tiny and broad maximum. This plot shows also the existence of the well-documented and typical polyelectrolyte upturn in the small q range discussed in more detail for other systems.[2,20,21]

To better understand the origin of this small and broad maximum, we have investigated different Na−Hy polyelectrolyte concentrations (5 g/L < C_P < 30 g/L) at different shear rates in the range of $\dot{\gamma} = 0.05$ s^{-1} to $\dot{\gamma} = 1600$ s^{-1} in both geometries, radial and tangential. At low shear rates and for all the concentrations, the peak is still hardly observable. When $\dot{\gamma}$ increases and is about 100 s^{-1}, a well-developed maximum emerges, and its position remains constant at higher shear rates. Figure 3 illustrates this behavior where $I(q)$ is plotted as a function of q at the different shear rates shown. One notes that the position of the scattering peak remains unchanged and shows that the equivalent interparticle distance at $C_P = 15$ g/L, $d = (2\pi/q) = 110$ Å, is unperturbed by the applied shear to the system. For comparison, we report in Figure 4 $I(q)$ vs q for the xanthan case ($C_P = 15$ g/L, "salt-free") at different shear rates. One observes a clear second-order peak that is enhanced as the shear rate is increased: its position is at about 2 times q_{max} corresponding to cylindrical

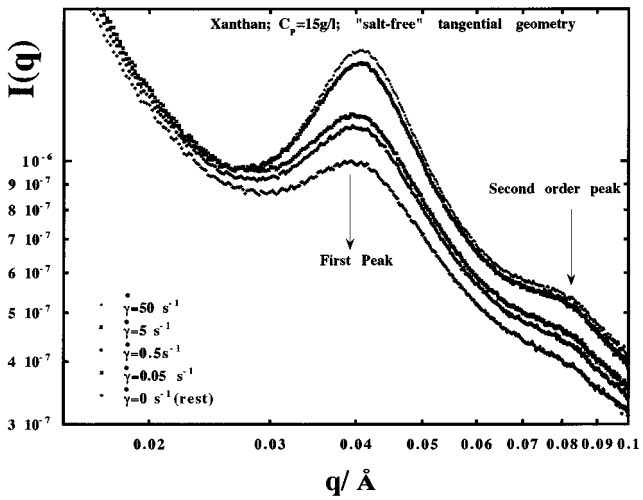

Figure 4. $I(q)$ vs q at rest and at different shown shear rates for xanthan sample at the "salt-free" polyelectrolyte concentration $C_P = 15$ g/L in the tangential geometry. Note the emergence of a second-order peak with increasing the shear.

organization of the particles ($1.9q_{max}$). Both figures were obtained in averaging the scattering intensity over 360° from the spectra in tangential configuration and for which the scattering is isotropic whatever the shear rate. This is not the case in the radial configuration. By increasing the shear rate, one observes an orientation of the system (alignment of the polyelectrolyte chains) in the (**k**v,**k**e) plane. This behavior is better illustrated in Figure 5 for the xanthan system. 2-D spectra labeled (a) to (d) correspond to the typical scattering pattern in radial configuration at different shear rates. At rest (zero shear rate or after stopping the shear) the intensity distribution at the peak position is isotropic. As the shear rate is increased, one observes an enhancement of the intensity in the vorticity direction which becomes well pronounced at high shear rates. We have plotted in Figure 6 the azimuthal intensity distribution at the peak position, in this configuration (radial). One observes an azimuthal narrowing of the peak at 90° and 270° which corresponds to the vorticity direction. On the other hand and at the same time, the intensity distribution at the peak position in the tangential configuration is isotropic whatever the shear rate. We show one example of a typical spectrum obtained at very high shear rate in Figure 5e. The intensity of this scattering ring in the (**k**∇,**k**e) plane corresponds to the scattering intensity of the peak in the (**k**v,**k**e) plane and along the e-direction. This result indicates an increase of the degree of the order in the solution as $\dot{\gamma}$ increases and corresponds to the alignment of the polymer chains in the velocity direction. The same behavior has been observed on the Na−Hy "salt-free" system but with a lower contrast. Similar observations were previously reported on, for instance, smectite clay colloids[42] and cellulose whiskers.[43]

Both results obtained on Na−Hy and on xanthan indicate a progressive development of an anisotropic structure corresponding to a preferential alignment of the ionic polymers in the direction of the shear when $\dot{\gamma}$ increases. It shows that the peak, which has been clearly observed at high shear rates, is indeed related to electrostatic interactions and reveals the expected polyelectrolyte nature of Na−Hy. It is also worth noting that shearing a neutral polymer system in the semidilute regime is well documented and leads to the so-called

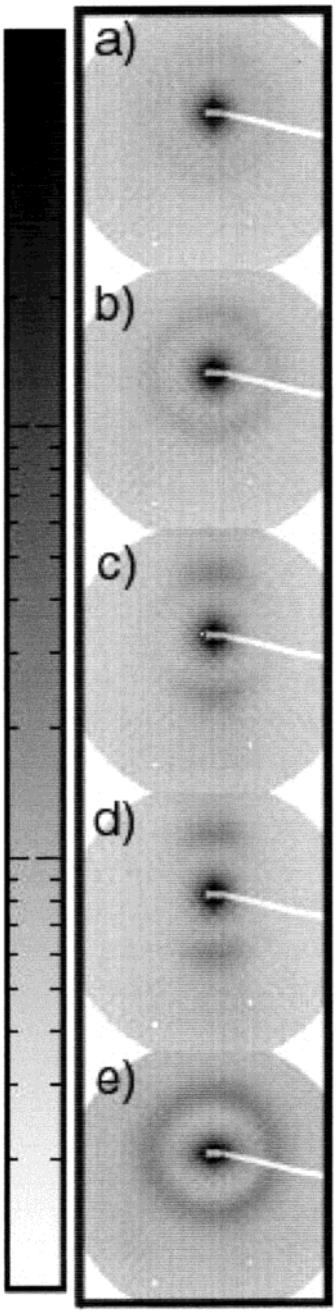

Figure 5. 2D SAXS pattern obtained on xanthan at $C_P = 15$ g/L in radial geometry at rest and at different shear rates: (a) $\dot{\gamma} = 0$ s^{-1}; (b) $\dot{\gamma} = 5$ s^{-1}; (c) $\dot{\gamma} = 50$ s^{-1}; (d) $\dot{\gamma} = 1600$ s^{-1}. Spectrum (e) corresponds to the tangential configuration at $\dot{\gamma} = 1600$ s^{-1}.

butterfly pattern (contour constituted of two lobes) for the isointensity curves as has been shown using SANS under shear.[44] Such a behavior of neutral polymer under shear is of course completely different from polyelectrolyte systems as has been clearly demonstrated in these experiments.

Conclusion

This paper discusses synchrotron SAXS data on Na−Hy and xanthan (for comparison) "salt-free" solutions at rest and under shear. Contrary to other radiation (light or neutrons), the use of high-brilliance SAXS enables the observation of the expected scattering peak in the Na−Hy polyelectrolyte systems. Indeed at zero shear rate, the scattered intensity $I(q)$ presents a very small maximum that becomes more intense as the shear is increased. These results show clearly, as opposed to neutral polymer systems, that the observed peak is related to electrostatic interactions magnified by the effect of shear. The position of the peak (q_{max}) remains at the same position at rest and at different shear rates. At high shear, the chains adopt a preferential orientation in the shear direction, leading the system to undergo a progressive change from isotropic to anisotropic phase clearly observed on the azimuthal narrowing of the peak. Compared to data obtained on other synthetic polyelectrolytes or polysaccharides, one may emphasize that the expected scattering peak in the Na−Hy system was not so far observed because of the weak electrostatic nature, the small intrinsic persistence length, and also the contrast when using neutrons or light scattering techniques. In this work, high-brilliance synchrotron was used to overcome the signal/noise ratio (contrast) and to highlight the electrostatic interactions of Na−Hy polyelectrolyte system. This has been achieved successfully using synchrotron radiation experiments and particularly magnified under shear. As for the xanthan case, a single peak exists at rest (the so-called polyelectrolyte peak), and the effect of shear induces a long-range order illustrated by the emergence of a second-order peak at high shear rates.

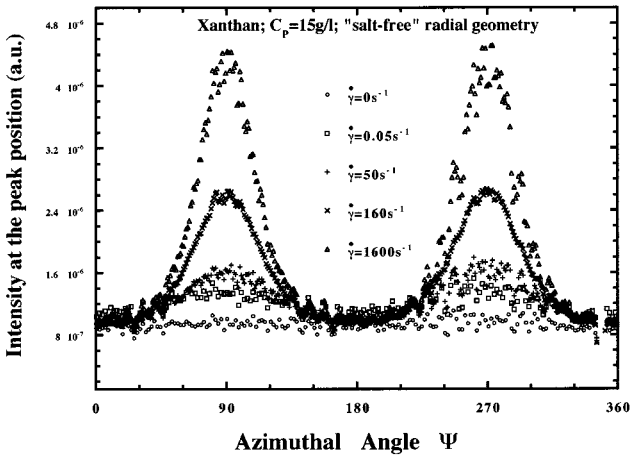

Figure 6. Variation of the circumferential integrated intensity at the peak position as a function of the azimuthal angle ψ for xanthan at $C_P = 15$ g/L in radial geometry at different shear rates from $\dot{\gamma} = 0$ s^{-1} to $\dot{\gamma} = 1600$ s^{-1}.

Acknowledgment. The authors gratefully acknowledge the ESRF for the use of the synchrotron facilities (allocation beamtime SC458). Marcos Villetti acknowledges the financial support from CAPES-Brazil during his PhD work in France.

References and Notes

(1) Katchalsky, A.; Alexandrowicz, Z.; Kedem, O. In *Chemical Physics of Ionic Solutions*; Conway and Barradas, Eds.; Wiley: New York, 1966.
(2) Ise, N. *Angew. Chem., Int. Ed. Engl.* **1986**, *25*, 323.
(3) Jannink, G. *Makromol. Chem. Macromol. Symp.* **1986**, *1*, 67.
(4) *Polyelectrolytes: Science and Technology*; Hara, M., Ed.; Marcel Dekker: New York, 1993.
(5) Mandel, M. In *Encyclopedia of Polymer Science and Engineering*, 2nd ed.; Mark, H. F., Bikales, N. M., Overberger, C. G., Menges, G., Eds.; Wiley: New York, 1988; Vol. II, p 739.
(6) Odijk, T. *J. Polym. Sci., Polym. Phys. Ed.* **1977**, *15*, 477.
(7) Barrat, J. L.; Joanny, J. F. *Europhys. Lett.* **1993**, *24*, 333.
(8) Stevens, M. J.; Kremer, K. *J. Chem. Phys.* **1995**, *4*, 103.

(9) Muthukumar, M. *J. Chem. Phys.* **1996**, *105*, 5183.
(10) de Gennes, P. G.; Pincus, P.; Velasco, R. M.; Brochard, F. *J. Phys. (Paris)* **1976**, *37*, 1461.
(11) Manning, G. S. *Rev. Biophys.* **1978**, *11*, 179.
(12) Joanny, J. F.; Leibler, L. *J. Phys. (Paris)* **1990**, *51*, 545.
(13) Vilgis, T. A.; Borsali, R. *Phys. Rev. A* **1991**, *A43*, 6857.
(14) Fuoss, R. M. *J. Polym. Sci., Phys. Ed.* **1948**, *3*, 603; *J. Polym. Sci., Phys. Ed.* **1949**, *4*, 96.
(15) Cohen, J.; Priel, Z.; Rabin, Y. *J. Chem. Phys.* **1988**, *88*, 7111.
(16) Yamanaka, J.; Matsuoka, H.; Kitano, H.; Ise, N. *J. Colloid Interface Sci.* **1991**, *134*, 92.
(17) Fukuda, K.; Suzuki, E.; Seimiya, T. Proceeding of the 50th Yamada Conference on Polyelectrolytes 1998 Inuyama, Japan.
(18) Fouissac, E.; Milas, M.; Rinaudo, M.; Borsali, R. *Macromolecules* **1992**, *25*, 5613.
(19) Yamanaka, J.; Araie, H.; Matsuoka, H.; Kitano, H.; Ise, N.; Yamaguchi, T.; Saeki, S.; Tsubokawa, M. *Macromolecules* **1991**, *24*, 3206; *Macromolecules* **1991**, *24*, 6156.
(20) Borsali, R.; Nguyen, H.; Pecora, R. *Macromolecules* **1998**, *31*, 1548.
(21) Ermi, B. D.; Amis, E. J. *Macromolecules* **1998**, *31*, 7378.
(22) Ise, N.; Okubo, T.; Yamamoto, K.; Kawai, H.; Hashimoto, T.; Fujimura, M.; Hiragi, Y. *J. Am. Chem. Soc.* **1980**, *102*, 7901.
(23) Kaji, K.; Urakawa, H.; Kanaya, T.; Kitamaru, R. *J. Phys. (Paris)* **1988**, *49*, 993.
(24) Nierlich, M.; Williams, C. E.; Boué, F.; Cotton, J. P.; Daoud, M.; Farnoux, B.; Jannink, G.; Picot, Cl.; Moan, M.; Wolff, C.; de Gennes, P. G. *J. Phys. (Paris)* **1979**, *40*, 701.
(25) Essafi, W.; Lafuma, F.; Williams, C. In *Macro-ion Characterization, From Dilute Solutions to Complex Fluids*; Schmitz, K. S.; Ed.; ACS Symp. Ser. N*o.* 548; American Chemical Society: Washington, DC, 1994; Chapter 21, p 278.
(26) Drifford, M.; Dalbiez, J. P. *J. Phys. Chem.* **1984**, *88*, 5368.
(27) Xiao, L.; Reed, W. F. *J. Chem. Phys.* 1991, **94**, 4568.
(28) Ghosh, S.; Li, X.; Reed, C. E.; Reed W. F. *Biopolymers* **1990**, *30*, 1101.
(29) Lin, S. C.; Li, W. I.; Schurr, M. J. *Biopolymers* **1978**, *17*, 1041.
(30) Sedlak, M.; Amis, E. J. *J. Chem. Phys.* **1992**, *96*, 817.
(31) Morfin, I.; Reed, W.; Rinaudo, M.; Borsali, R. *J. Phys. II* **1994**, *4*, 1001.
(32) Forster, S.; Schmidt, M.; Antonietti, M. *Polymer* **1990**, *31*, 781.
(33) Hagenbuchle, M. *Physica A* **1990**, *169*, 29.
(34) Wang, L.; Bloomfield, V. *Macromolecules* **1991**, *24*, 5791.
(35) Schmitz, K. *Dynamic Light Scattering by Macromolecules*; Academic Press: New York, 1990.
(36) Borsali, R.; Rinaudo, M.; Noirez, L. *Macromolecules* **1995**, *28*, 1085.
(37) Milas, M.; Rinaudo, M.; Duplessix, R.; Borsali, R.; Lindner, P. *Macromolecules* **1995**, *28*, 3199.
(38) Asakawa, H.; Seito, S.; Yanagi, M.; Fukushima, S.; Mitsui, T. *J. Soc. Cosmet. Chem. Jpn.* **1988**, *22*, 35.
(39) Cleland, R. L.; Wang, J. L. *Biopolymers* **1970**, *9*, 799; *Biopolymers* **1984**, *23*, 647.
(40) Villetti, M.; Borsali, R. Manuscript in preparation.
(41) Bösecke, P.; Diat, O. *J. Appl. Crystallogr.* **1997**, *30*, 867.
(42) Ramsay, J. D. F.; Lindner *J. Chem. Soc., Faraday Trans.* **1993**, *89*, 4207.
(43) Ebeling, T.; Paillet, M.; Borsali, R.; Diat, O.; Dufresne, A.; Cavaillé, J. Y.; Chanzy, H. *Langmuir* **1999**, *19*, 6123.
(44) Morfin, I.; Lindner, P.; Boué, F. *Macromolecules* **1999**, *32*, 7208.

MA000971Z